Composites: Part B 58 (2014) 43–53

Contents lists available at ScienceDirect

Composites: Part B

journal homepage: www.elsevier.com/locate/compositesb

Nano-epoxy resins containing electrospun carbon nanofibers and the resulting hybrid multi-scale composites

Qi Chen [a], Weidong Wu [b,*], Yong Zhao [a], Min Xi [a], Tao Xu [a,b], Hao Fong [a,*]

[a] Department of Chemistry and Applied Biological Sciences, South Dakota School of Mines and Technology, Rapid City, SD 57701, USA
[b] The Key Laboratory of Beijing City on Preparation and Processing of Novel Polymer Materials, Beijing University of Chemical Technology, Beijing 100029, China

ARTICLE INFO

Article history:
Received 10 March 2013
Received in revised form 8 September 2013
Accepted 25 October 2013
Available online 6 November 2013

Keywords:
A. Polymer–matrix composites (PMCs)
A. Carbon fiber
B. Mechanical properties

ABSTRACT

For the first time, electrospun carbon nanofibers (ECNFs, with diameters and lengths of ~200 nm and ~15 μm, respectively) were explored for the preparation of nano-epoxy resins; and the prepared resins were further investigated for the fabrication of hybrid multi-scale composites with woven fabrics of conventional carbon fibers *via* the technique of vacuum assisted resin transfer molding (VARTM). For comparison, vapor growth carbon nanofibers (VGCNFs) and graphite carbon nanofibers (GCNFs) were also studied for making nano-epoxy resins and hybrid multi-scale composites. Unlike VGCNFs and GCNFs that are prepared by bottom-up methods, ECNFs are produced through a top-down approach; hence, ECNFs are more cost-effective than VGCNFs and GCNFs. The results indicated that the incorporation of a small mass fraction (*e.g.*, 0.1% and 0.3%) of ECNFs into epoxy resin would result in substantial improvements on impact absorption energy, inter-laminar shear strength, and flexural properties for both nano-epoxy resins and hybrid multi-scale composites. In general, the reinforcement effect of ECNFs was similar to that of VGCNFs, while it was higher than that of GCNFs.

1. Introduction

Carbon nanofibers (CNFs) have been extensively investigated as nanoscale reinforcement agents for the fabrication of polymer nanocomposites due to superior strength, high stiffness, and excellent electrical/thermal properties [1]. However, to uniformly disperse/distribute CNFs into polymer resins remains as a technological challenge, since CNFs tend to form agglomerates that would act as structural defects in the resulting nanocomposites and thus limit the improvement of mechanical properties. The surface functionalization of CNFs is crucial to resolve/mitigate the problem, because the surface wettability/reactivity of CNFs, as well as the interfacial bonding strength between CNFs and polymer resins, could be considerably improved *via* the introduction of functional groups on the surface of nanofibers [2]. Among various approaches for the surface functionalization of CNFs, an appealing one is through covalent bonding of linker molecules to the nanofiber surface. In the recent years, there have been numerous studies on the development of polymer nanocomposites reinforced with different types of CNFs (*e.g.*, vapor-grown CNFs and graphite CNFs); and significant improvements on mechanical properties have been reported through successful surface functionalization of those CNFs [3–9].

An important application of nanoscale reinforcement agents is to prepare nano-resins for further fabrication of hybrid multi-scale composites. It is known that the out-of-plane properties of fiber reinforced polymer composites (FRPs) are dominated by resin matrices, and they are substantially lower than the in-plane properties. Numerous investigations have indicated that the properties (particularly out-of-plane properties) of hybrid multi-scale FRPs, in which nanoscale reinforcement agents are dispersed as the second phase of matrices, can be improved substantially [10–13]. Various types of nanoscale materials including graphite nanofibers, carbon nanotubes/nanofibers (CNTs/CNFs), organoclays, and silica nanoparticles have been studied to prepare nano-resins for the reinforcement of matrix-rich inter-laminar regions [14–20]. The techniques of resin transfer molding (RTM) and vacuum assisted resin transfer molding (VARTM) are commonly adopted for the fabrication of hybrid multi-scale FRPs [21–24]. It is noteworthy that Wichmann et al. [13] prepared three types of multi-scale FRPs containing fumed silica, carbon black, and CNTs, respectively, by the RTM technique; their results indicated that the nanometer-sized reinforcement would not be filtered by the conventional fibers, while the resulting hybrid multi-scale FRPs exhibited substantially improved mechanical properties. However, only limited research endeavors have been devoted to the development of two-phase

* Corresponding authors. Tel.: +86 10 64434860; fax: +86 10 64433964 (W. Wu), tel.: +1 605 394 1229; fax: +1 605 394 1232 (H. Fong).
E-mail addresses: wuweidong@mail.buct.edu.cn (W. Wu), Hao.Fong@sdsmt.edu (H. Fong).

1359-8368/$ - see front matter © 2013 Elsevier Ltd. All rights reserved.
http://dx.doi.org/10.1016/j.compositesb.2013.10.048

nano-resins and three-phase hybrid multi-scale FRPs with electrospun nanofibers [25–28].

The materials-processing technique of electrospinning provides a viable approach for convenient preparation of polymeric, ceramic, and carbonaceous fibers (commonly known as "electrospun nanofibers") with diameters in the range from nanometers to micrometers [29]. In general, electrospun carbon nanofibers (ECNFs) can be prepared *via* thermal treatments (*i.e.*, stabilization in air followed by carbonization in inert environment) of their precursors such as electrospun polyacrylonitrile (PAN) nanofibers. Unlike CNTs/CNFs and graphite nanofibers that are prepared by bottom-up methods, ECNFs are produced through a top-down approach, resulting in cost-effective nanofibers that are also easy for being processed into applications. Recently, we have reported that ECNFs (in the form of overlaid mat) could be sandwiched or surface-attached onto woven fabrics of conventional carbon fibers (CFs) for the fabrication of hybrid multi-scale composites; and these composites demonstrated considerably higher inter-laminar shear strength and flexural properties than the control samples (*i.e.*, the traditional laminated composites made of CF fabrics without ECNFs) [30,31].

In this study, shortened ECNFs surface-functionalized with hexanediamine (ECNFs-HDA) were incorporated (at low mass fractions of 0.1%, 0.3%, and 0.5%) into an epoxy resin for reinforcement and/or toughening purposes; and the innovative nano-epoxy resins were further used for the fabrication of carbon fibers reinforced polymer composites (CFRP). Fig. 1 is a schematic representation showing the CNFs-containing epoxy resins as the matrix materials for the fabrication of CFRP laminates *via* the VARTM technique. The effects of ECNFs-HDA incorporation on the mechanical properties of two-phase nano-epoxy resins and three-phase CFRP composites were investigated, and the results were compared to those acquired from the nano-epoxy resins and CFRP composites made from the vapor-grown carbon nanofibers (VGCNFs) surface-functionalized with HDA (VGCNFs-HDA) and the graphite carbon nanofibers (GCNFs) surface-functionalized with HDA (GCNFs-HDA).

2. Experimental

2.1. Materials

The epoxy resin of SC-15A and the associated hardener of SC-15B were supplied by the Applied Poleramic Inc. (Benicia, CA). The PAN used in this study were the Special Acrylic Fibers (SAF 3K fibers) provided by the Courtaulds, Ltd. (Essex, UK). The SAF 3K fibers were made of a PAN copolymer with 92.8 wt.% of acrylonitrile, 1.2 wt.% of itaconic acid, and 6.0 wt.% of methyl acrylate, and they were in the form of bundle with 3000 individual fibers. The chemicals of acetone, nitric acid, hexanediamine (HDA), and *N,N*-dimethylformamide (DMF) were purchased from the Sigma–Aldrich Co. (St. Louis, MO). GCNFs (Sigma–Aldrich Co., MO) and VGCNFs (Pyrograf III PR-24, the Applied Science Inc., OH) were studied as the comparison nano-reinforcement agents to fabricate nano-epoxy resins and hybrid multi-scale composites. The woven fabrics of T300® CFs were produced by the Toray Industries, Inc. (Tokyo, Japan).

The SEM images of A, B, and C in Fig. 2 were acquired from the as-received T300® CFs, VGCNFs, and GCNFs, respectively. The T300® CFs had diameters of ~7 μm, while the VGCNFs and GCNFs had diameters of ~170 and 80 nm, respectively. The average length of VGCNFs was ~10 μm, while the average length of GCNFs was ~50 μm; hence, the average aspect ratio (*i.e.*, the average ratio of length to diameter) of VGCNFs and GCNFs were 59 and 625, respectively. As shown in Fig. 2C, the GCNFs appeared more agglomerated than the VGCNFs probably due to smaller diameters (and the concomitant larger specific surface areas) and higher aspect ratios [32,33].

2.2. Preparation of electrospun carbon nanofibers (ECNFs)

The ECNFs were prepared *via* electrospinning of PAN copolymer nanofibers followed by thermal treatments of stabilization and carbonization. The preparation procedures/conditions and the detailed characterizations/evaluations were reported in our previous publication [30]. In this study, the prepared ECNFs (in the form of overlaid mat with the thickness of ~15 μm) were first cut into small pieces with length and width of 1–2 mm; these small pieces were then immersed in distilled water for being sonicated by using a Branson (Model 2510) sonifier for 2 h. Thereafter, the mixture was mechanically stirred by using a Heidolph RZR 50 Heavy Duty Stirrer for 48 h to obtain the shortened ECNFs with diameters and lengths of ~200 nm and ~15 μm, respectively. The prepared short ECNFs with the aspect ratios of ~75 are shown in Fig. 2D.

2.3. Surface-functionalization of CNFs with HDA

VGCNFs, GCNFs, and (the prepared short fibers of) ECNFs were first heated in 3 M nitric acid at 115 °C for 4 h and then washed

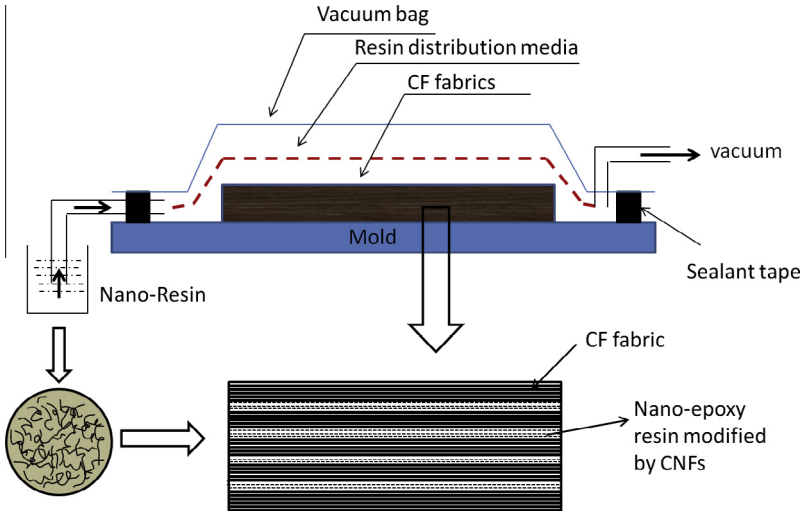

Fig. 1. A schematic showing the fabrication of hybrid multi-scale CFRP composites using nano-epoxy resins containing HDA surface-functionalized CNFs *via* the VARTM technique.

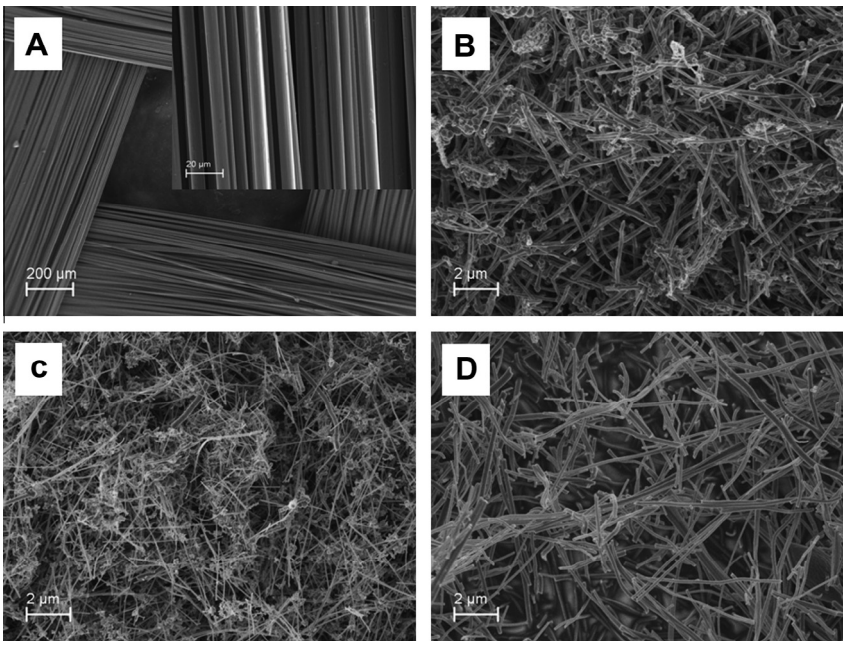

Fig. 2. SEM images showing the representative morphologies of (A) T300® CF fabrics (with the inset showing a microfiber bundle in the fabric), (B) VGCNFs, and (C) GCNFs, as well as (D) ECNFs after being shortened.

with distilled water until the filtrate reached a *p*H value of 5.5–6.5; subsequently, they were dried at 80 °C for 12 h. The oxidized VGCNFs, GCNFs, and ECNFs were then reacted with excess amount of HDA at 100 °C in nitrogen for 80 h. After being rinsed with acetone for several times, the HDA surface-functionalized CNFs (*i.e.*, ECNFs-HDA, VGCNFs-HDA, and GCNFs-HDA) were dried at 80 °C for 12 h.

2.4. Development of nano-epoxy resins

Nano-epoxy resins were developed by the method of solvent casting. Each type of HDA surface-functionalized CNFs was first mixed with acetone (mass ratio of CNFs/acetone: 1/5) in a glass bottle; the mixture was then ultra-sonicated for 30 min. Subsequently, the SC-15A epoxy resin was added into the mixture at 80 °C, and the mixture was then mechanically stirred at 400 rpm for 24 h until the solvent was removed completely and a uniform mixture was obtained. Thereafter, the SC-15B hardener was added into the mixture; and the mass ratio of the epoxy resin *versus* the hardener was set at 100/30. After being degassed, the mixture was poured into an aluminum mold (treated with Frekote® 700-NC mold release agent, and pre-heated at 70 °C) followed by being cured initially at 60 °C for 2 h and then at 110 °C for 5 h to obtain three types of nano-epoxy panels with length, width, and thickness being 100, 100, and 6 mm, respectively. Finally, specimens with the dimensions of $64 \times 12.7 \times 6\ mm^3$ were cut from the panels for Izod impact test according to ASTM D256, specimens with the dimensions of $100 \times 12.7 \times 6\ mm^3$ were cut for three-points bending test according to ASTM D790, and the dog-bone shaped specimens for tensile test were prepared according to ASTM D638.

2.5. Fabrication of hybrid multi-scale CFRP composites

Each of the three nano-epoxy resins was first infused into a vacuum bag containing six plies of woven CF fabrics using the VARTM technique, as schematically shown in Fig. 1. It is noteworthy that, even with a small amount of nanofibers (including ECNFs-HDA, VGCNFs-HDA, and GCNFs-HDA) incorporated into epoxy resin, a considerable increase of viscosity would be observed; to improve the fluidity, the colloidal suspension was kept at 50 °C, and the vacuum of ~27 mmHg was applied during the initial curing at room temperature for 24 h. The obtained composites were further cured in an oven at 110 °C for 5 h before being characterized and evaluated. For comparison, the conventional laminated composite made from six plies of woven CF fabrics and neat epoxy resin (without any CNFs) was also fabricated and evaluated. Finally, specimens with the dimensions of $64 \times 12.7 \times 1.6\ mm^3$ were cut from the composite panels for Izod impact test according to ASTM D256; specimens with the dimensions of $50.8 \times 12.7 \times 1.6\ mm^3$ were cut for three-points bending test according to ASTM D790, and specimens with the dimensions of $8 \times 4 \times 1.6\ mm^3$ were cut for short beam test according to ASTM D2344.

2.6. Characterization and evaluation

A Zeiss Supra 40 VP field-emission scanning electron microscope (SEM) was employed to examine the morphologies of fibers as well as the fracture surfaces of composites. Prior to SEM examinations of fracture surfaces, specimens were sputter-coated with gold to avoid charge accumulations. Fourier transform infrared (FT-IR) spectra of as-prepared ECNFs, oxidized ECNFs, and ECNFs-HDA were acquired from a Bruker Tensor-27 FT-IR spectrometer equipped with a liquid nitrogen cooled mercury-cadmium-telluride (MCT) detector; the samples were prepared by grinding and then pressing the fibers with KBr, and the FT-IR spectra were acquired by scanning the samples (64 scans) from 600 to 4000 cm^{-1} with a resolution of 4 cm^{-1}.

Measurements of mechanical properties were conducted at room temperature. The Izod impact test was carried out using a Tinius Olsen impact tester (Impact 104) according to ASTM D256. The standard tension test was performed according to ASTM D638 at a strain rate of 1 mm/min using a computer-controlled universal mechanical testing machine (QTEST™/10, MTS Systems, USA). The three-point bending tests with the span distance of 60 mm for the specimens of nano-epoxy resins and with the span distance of 25.4 mm for the specimens of laminated composites

were conducted according to ASTM D790, and the specimens were fractured at the strain rate of 0.01 mm/mm/min. According to ASTM D2344, the short-beam test was carried out at the span-to-thickness ratio of 4 and the cross-head speed of 1 mm/min. Three specimens of each sample were evaluated, and mean values and the associated standard deviations of mechanical properties were calculated.

3. Results and discussion

3.1. Surface functionalization

As schematically shown in Fig. 3, nitric acid and HDA were used for oxidation and functionalization on the surfaces of the three types of CNFs, respectively. The representative SEM images of the obtained ECNFs-HDA, VGCNFs-HDA, GCNFs-HDA are shown in Fig. 4A–C. Compared to the CNFs in Fig. 1B–D, no appreciable difference on morphology was identified for ECNFs and VGCNFs before and after surface oxidation and functionalization. However, more agglomerates were observed in Fig. 4C; this was probably because GCNFs had more edge carbon atoms (and/or surface reactive sites) than ECNFs and VGCNFs. Hence, more HDA molecules could be bonded to the fiber surface, resulting in linking more GCNFs and forming more agglomerates.

FT-IR spectra of the as-prepared, oxidized, and surface-functionalized ECNFs are shown in Fig. 5. The band centered at 1580 cm^{-1} in the spectrum of as-prepared ECNFs is assigned to the stretching and bending mode of C=C [34]. FT-IR spectra of the oxidized ECNFs (H-ECNFs) and ECNFs-HDA have the same band around 1580 cm^{-1}, suggesting that the structures of nanofibers are not distinguishably affected by the treatments with nitric acid and HDA; and this is consistent with SEM observations. A new band in the spectrum of H-ECNFs appears around 1620 cm^{-1}, which is attributed to carboxyl (–COOH) groups on fiber surface [34]. Upon surface functionalization of H-ECNFs with HDA, amide groups emerge as evidenced by a relatively broad band around 1655 cm^{-1}. The spectrum of ECNFs-HDA also has bands around 2936 and 2843 cm^{-1}, which are due to the stretching modes of C—H in the alkyl component [35]. Additionally, the FT-IR spectrum of ECNFs has a broad band centered at 3440 cm^{-1} that is attributed to –OH groups on the surface of nanofibers. Meantime, the carboxyl and amino groups (generated from the treatments of nitric acid and HDA) can also result in bands around such a wavenumber. Hence, variations of the band centered at 3440 cm^{-1} can be used as an indication for oxidation and functionalization on the surface of ECNFs. Through comparison of FT-IR spectra acquired from ECNFs, H-ECNFs, and ECNFs-HDA, it is evident that the absorption/band

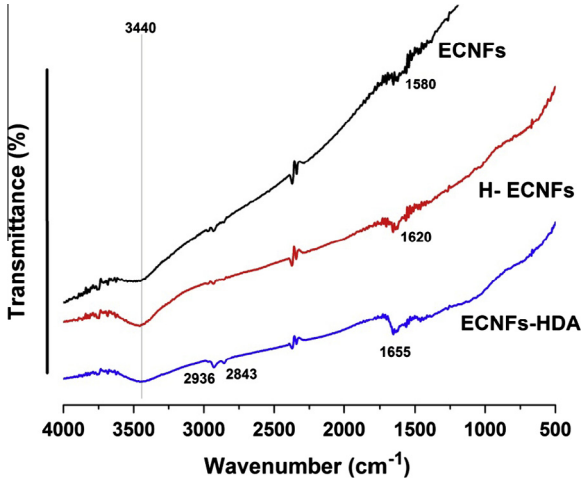

Fig. 5. FT-IR spectra of ECNFs, oxidized ECNFs (H-ECNFs), and ECNFs-HDA.

between 3000 and 3750 cm^{-1} for ECNFs-HDA is strengthened, suggesting that the oxidation and amidation reactions have occurred as shown in Fig. 3. The similar oxidation and amidation reactions can also occur to VGCNFs and GCNFs.

3.2. Mechanical properties

3.2.1. Mechanical properties of nano-epoxy resins

The impact, three-point bending, and tensile tests on the nano-epoxy resins containing low mass fractions (*i.e.*, 0.1%, 0.3%, and 0.5%) of ECNFs-HDA, VGCNFs-HDA, and GCNFs-HDA were performed, and the acquired results are shown in Fig. 6. The control sample was the neat epoxy resin without any nano-reinforcement agent.

3.2.2. Impact and tensile properties

As shown in Fig. 6A–B, the incorporation of ECNFs-HDA, VGCNFs-HDA, or GCNFs-HDA into epoxy resin improved the impact absorption energy and tensile strength of the resulting nano-epoxy resins. The impact absorption energy and tensile strength of neat epoxy resin (mean ± standard deviation, $n = 3$) was (3.00 ± 0.51) KJ/m^2 and (44.4 ± 0.7) MPa. For the nano-epoxy resins with 0.5% of ECNFs-HDA, VGCNFs-HDA, and GCNFs-HDA, the respective values of impact absorption energy were (3.52 ± 0.52), (3.44 ± 0.94), and (3.60 ± 0.51) KJ/m^2; hence, the improvements were 17.3%, 14.7%, and 20.0%, respectively. For

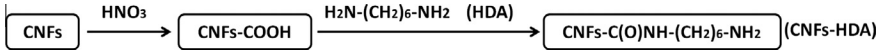

Fig. 3. A schematic showing the surface oxidation and functionalization of CNFs.

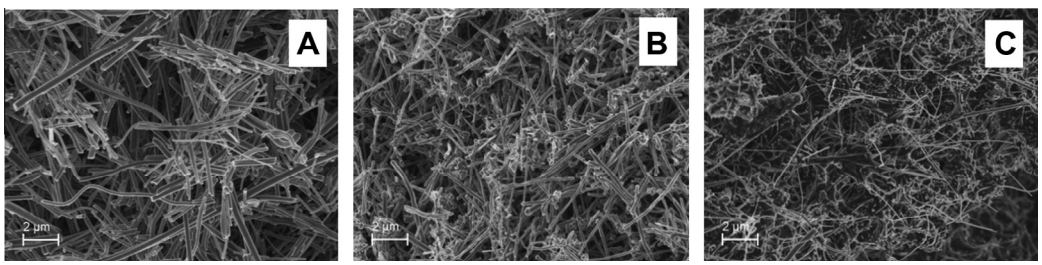

Fig. 4. SEM images showing the representative morphologies of HDA surface-functionalized CNFs: (A) ECNFs-HDA, (B) VGCNFs-HDA, and (C) GCNFs-HDA.

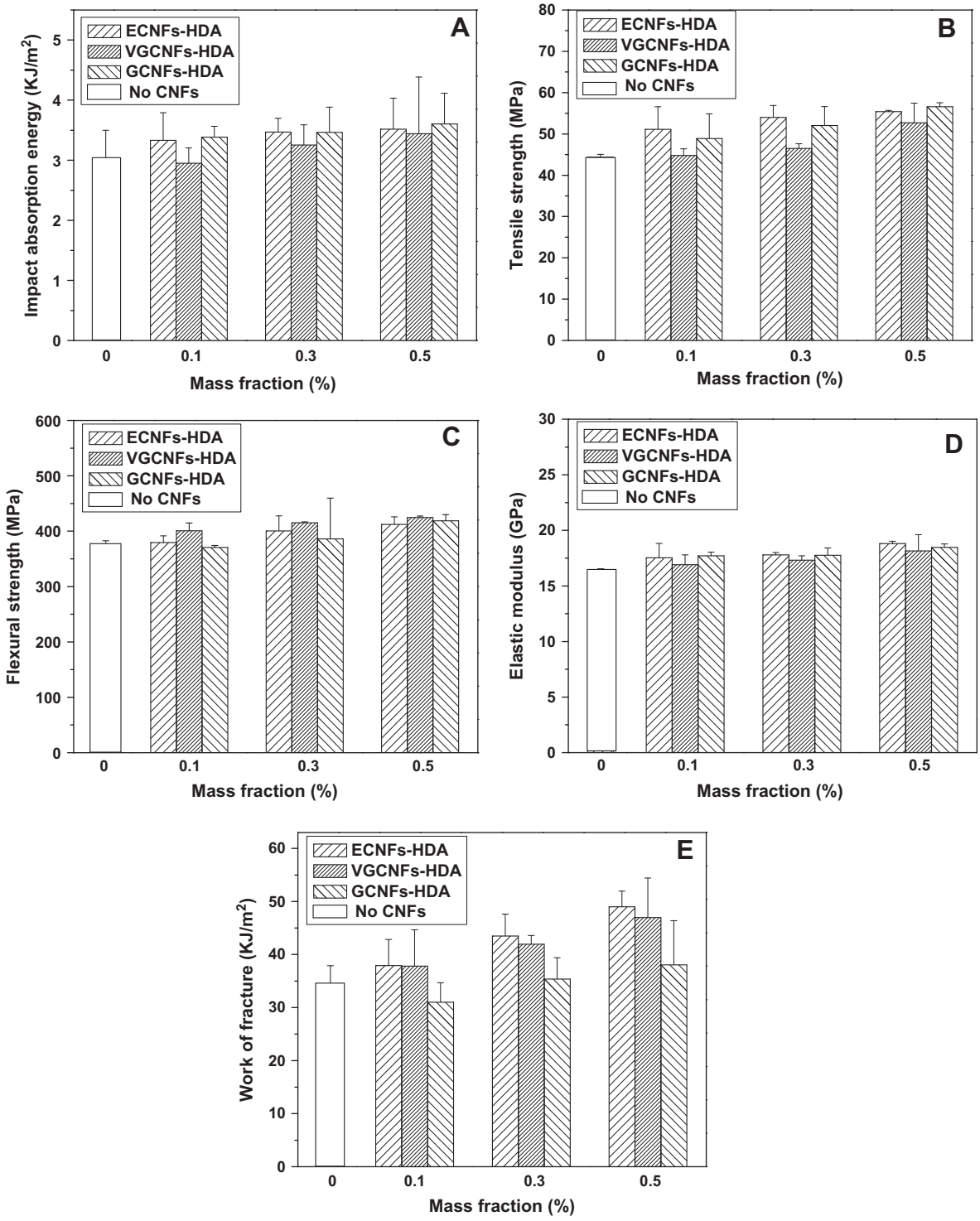

Fig. 6. Impact absorption energy (A), tensile strength (B), flexural strength (C), elastic modulus (D), and work of fracture (E) of neat epoxy resin (control sample) and the nano-epoxy resins containing varied mass fractions (*i.e.*, 0.1%, 0.3%, and 0.5%) of ECNFs-HDA, VGCNFs-HDA, and GCNFs-HDA.

tensile strength, the respective improvements were 22.5%, 18.7%, and 27.5%.

3.2.3. Flexural properties

The flexural strength (Fs), elastic modulus (Ey), and work of fracture (WOF) of nano-epoxy resins reinforced with ECNFs-HDA, VGCNFs-HDA, and GCNFs-HDA were studied, and the values were calculated based upon the following equations:

$$\mathrm{Fs} = 3FL/2bh^2$$

$$\mathrm{Ey} = L^3F_1/4fbh^3$$

$$\mathrm{WOF} = A/bh$$

where F is the applied load (N) at the highest point of load–displacement curve, L is the span distance (60.0 mm), b is the width

of specimen, and h is the thickness of specimen, F_1 is the load (N) at a convenient point in straight-line portion of the trace, f is the displacement (mm) of the test specimen at load F_1. A (J) is the work done by the applied load to deflect and fracture the specimen, corresponding to the area under the load–displacement curve. WOF is the work of fracture in KJ/m^2.

As shown in Fig. 6C–D, the neat epoxy resin exhibited the Fs and Ey values of (374.8 ± 7.9) MPa and (16.4 ± 0.1) GPa, while the Fs and Ey values of nano-epoxy resins increased slightly with increasing the amount of all three types of CNFs. Incorporation of ECNFs-HDA resulted in 10.0% and 14.6% increase of Fs and Ey for the nano-epoxy resin at the mass fraction of 0.5%, while VGCNFs-HDA showed 13.3% and 11.0% increases and GCNFs-HDA showed 11.7% and 12.8% increases. Hence, there were no appreciable differences on the Fs and Ey of the nano-epoxy resins reinforced with ECNFs-HDA, VGCNFs-HDA, and GCNFs-HDA. The WOF of the nano-epoxy resins reinforced with ECNFs-HDA, VGCNFs-HDA, and GCNFs-HDA is shown in Fig. 6E. The nano-epoxy resin with ECNFs-HDA showed the highest WOF value. The WOF value of the neat resin was (34.1 ± 3.8) KJ/m^2. For the nano-epoxy resins with 0.5% ECNFs-HDA, VGCNFs-HDA, and GCNFs-HDA, the values of WOF were increased to (49.0 ± 2.9), (47.0 ± 7.4), and (38.1 ± 8.3) KJ/m^2, respectively. Thus, ECNFs-HDA led to 43.7% improvement; for comparison, VGCNFs-HDA and GCNFs-HDA led to 40.8% and 11.7% improvements, respectively. The WOF improvement resulted from GCNFs-HDA was lower than that from ECNFs-HDA or VGCNFs-HDA, because GCNFs-HDA had smaller diameters and larger aspect ratios; hence, they could form more agglomerates that would be mechanical weak points (*i.e.*, structural defects).

3.2.4. Mechanical properties of hybrid multi-scale CFRP composites made from nano-epoxy resins with surface-functionalized CNFs

Impact absorption energy, inter-laminar shear strength, and flexural strength of hybrid multi-scale CFRP composites made from nano-epoxy resins with surface-functionalized CNFs (*i.e.*, ECNFs-HDA, VGCNFs-HDA, and GCNFs-HDA) were investigated, and the acquired data are shown in Fig. 7A–C. The control sample was the conventional CFRP composite made from the neat epoxy resin. With the increase of ECNFs-HDA, VGCNFs-HDA, and GCNFs-HDA amounts up to 0.3%, the impact absorption energy, inter-laminar shear strength, and flexural strength also increased. For the control sample, the values of impact absorption energy, inter-laminar shear strength, and flexural strength were (35.0 ± 10.5) KJ/m^2, (32.2 ± 1.8) MPa, and (479.6 ± 33.2) MPa, respectively. For the CFRP/nano-epoxy composites containing 0.3% ECNFs-HDA, VGCNFs-HDA, and GCNFs-HDA, the respective values of impact absorption energy were (62.7 ± 13.1), (57.7 ± 12.0), and (57.6 ± 7.5) KJ/m^2, which were improved by 79.1%, 64.9%, and 64.6%, respectively; the respective values of inter-laminar shear strength were (45.8 ± 7.1), (38.3 ± 3.5), and (37.4 ± 1.3) MPa, which were improved by 42.2%, 18.9%, and 16.1%, respectively; the respective values of flexural strength were (545.0 ± 9.5), (567.3 ± 21.8), and (552.6 ± 44.8) MPa, which were improved by 13.6%, 18.3%, and 15.2%, respectively. However, when the amounts of ECNFs-HDA, VGCNFs-HDA, and GCNFs-HDA in nano-epoxy resins were increased to 0.5%, the impact absorption energy, inter-laminar shear strength, and flexural strength decreased, and the values were even lower than those of the control sample; this was likely due to the following two reasons: (1) the formation of nanofiber agglomerates during the infusion process when the amount of nanofibers in nano-epoxy resins was high; and the agglomerates would act as mechanical weak points (*i.e.*, structural defects) in composites, leading to the decrease of mechanical properties; (2) the filtering of ECNFs-HDA, VGCNFs-HDA, and GCNFs-HDA by the CF fabric when the amount of nanofibers was above 0.3%, resulting in inhomogeneous dispersion of nanofibers in hybrid multi-scale CFRP composites [36].

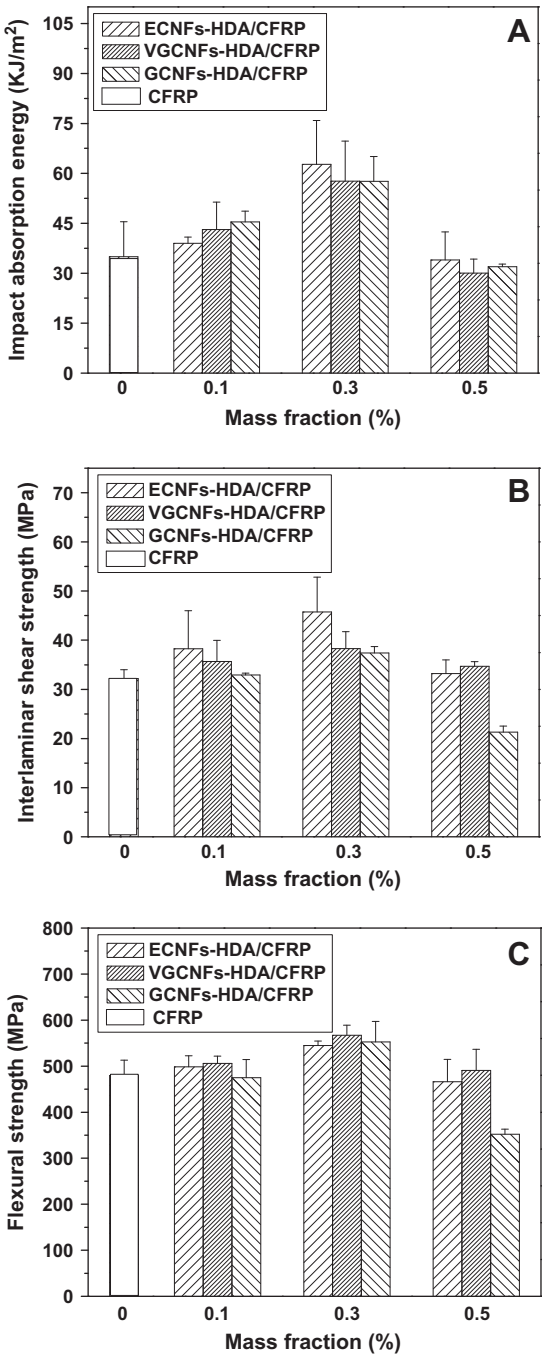

Fig. 7. Impact absorption energy (A), inter-laminar shear strength (B), and flexural strength (C) of the CFRP composites made from the neat epoxy resin (control sample) and the nano-epoxy resins containing varied mass fractions (*i.e.*, 0.1%, 0.3% and 0.5%) of ECNFs-HDA, VGCNFs-HDA, and GCNFs-HDA.

3.3. Reinforcement mechanisms

3.3.1. Nano-epoxy resins

CNFs have high strength, modulus/stiffness, and excellent electrical and thermal property; however, their application for reinforcement is also upon the interfacial properties between the fibers and matrices. This is because the interfacial bonding strength primarily determines the failure mode of composites.

When the interfacial bonding strength is high, matrix failure will be the main mode; when the interfacial bonding strength is low, the fiber-matrix interface will be the weakest part when a load is applied [37–40]. Numerous research endeavors have been devoted to the improvement of interfacial properties of carbon fibers, and many surface treatment techniques have been studied. The surface treatment methods such as oxidation and etching can considerably improve the interfacial bonding adhesion [40]. According to the composite theory, the reinforcement of CNFs for nano-epoxy resins is attributed to the higher strength and modulus of CNFs than those of epoxy resin. The higher mass fraction of CNFs, the higher strength and modulus of the resulting composite resins are expected to obtain. However, the reinforcement effect of CNFs can only be achieved if an effective load transfer from resin matrix to fibers is available. For mechanical properties of the nano-epoxy resins reinforced with CNFs, the nanofiber-matrix interfacial bonding strength is important; the high bonding strength would result in high strength and modulus of nano-epoxy resins. In this study, the oxidation and functionalization on the surfaces of CNFs improved the interfacial bonding strength between fibers and matrix, and led to increases of mechanical properties of the nano-epoxy resins reinforced with low mass fractions (0.1%, 0.3%, & 0.5%) of ECNFs-HDA, VGCNFs-HDA, and GCNFs-HDA. The ECNFs-HDA exhibited the strongest reinforcement effect while VGCNFs-HDA had the weakest reinforcement effect.

Regarding physical properties, GCNFs have the smallest diameters (and the concomitant largest specific surface area) and highest aspect ratio; hence, electrostatic and/or van der Waals forces among GCNFs are the strongest among the three types of CNFs. In consequence, GCNFs are easier to form agglomerates, hindering them to be uniformly dispersed in resin matrices and limiting the improvement on mechanical properties of the nano-epoxy resins. On the other hand, since higher specific surface area would also lead to more reactive carbon atoms, it is speculated that GCNFs could form more bonds with surface-functionalization agent of HDA than VGCNFs and ECNFs. Fracture surfaces of the nano-epoxy resins can provide valuable information on fracture mechanism and interfacial bonding strength. The fracture surfaces of impact test specimens were examined by SEM (Fig. 8). The relatively smooth surface with oriented fracture lines initiated from sites of crack growth was observed on the fracture surface of the neat epoxy resin (Fig. 8A). The nano-epoxy resins containing 0.5% ECNFs-HDA, VGCNFs-HDA, and GCNFs-HDA (Fig. 8B–D) had rough features on their fracture surfaces, and jagged, short, and multiplane fracture lines were observed; this indicated that the crack fronts were deflected and kinked during growth. Therefore, the main function of CNFs in nano-epoxy resins was to deflect the propagating cracks and force the crack growth to deviate from the existing fracture plane. Additional energy was then necessitated to continuously drive the growth of cracks, since the creation of additional fracture surface area would consume energy. Increasing the mass fraction of CNFs from 0.1% to 0.3% and then to 0.5% resulted in higher degree of deflecting effect, which further improved the mechanical properties.

The SEM images of fracture surfaces of nano-epoxy resins impregnated with ECNFs-HDA, VGCNFs-HDA, and GCNFs-HDA also showed that the CNFs were dispersed in epoxy resin uniformly and exhibited an improved interphase with epoxy matrix; furthermore, it could be found that ECNFs-HDA had the highest interfacial bonding strength with epoxy matrix, while VGCNFs had the lowest interfacial bonding strength with epoxy (Fig. 8B–D). Note that during the epoxy-curing process, some partial agglomerates were formed on fracture surface of the nano-epoxy resin containing 0.5% VGCNFs-HDA due to weak interfacial bonding strength. The micromechanics-based model for low mass fractions of reinforcements developed by Shi and coworkers [41] indicated that the partial agglomeration of nano-reinforcement agents in polymer matrix would decrease mechanical properties of the composite considerably, and such a model could explain that the incorporation of VGCNFs-HDA exhibited lower mechanical properties than the incorporation of ECNFs-HDA or GCNFs-HDA. Additionally, the fiber pull-out and/or de-bonding could be identified in the SEM images; this also had negative effect on the improvement of mechanical properties for the nano-epoxy resins.

The following Eq. (1) based on the modified rule of mixture was adopted to calculate the tensile strength and elastic modulus for

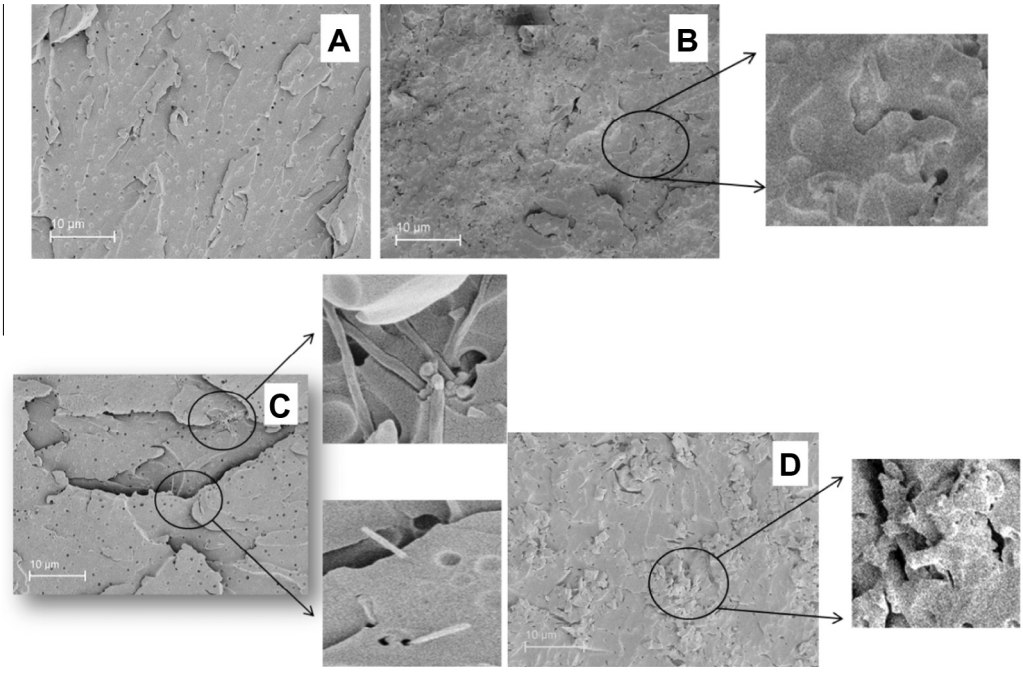

Fig. 8. SEM images showing the typical fracture surfaces of neat epoxy resin (A), the nano-epoxy resins with 0.5% ECNFs-HDA (B), VGCNFs-HDA (C), and GCNFs-HDA (D).

the nano-epoxy resins containing randomly/uniformly dispersed CNFs [42].

$$Y_c = Y_f(1 - \alpha_c/\alpha_f)\varphi + Y_m(1 - \varphi) \quad (1)$$

where Y_c, Y_m, and Y_f are the strength or modulus of nano-epoxy resin, epoxy matrix, and fibers, respectively; and φ is the volume fraction of fibers. The parameters of α_c and α_f are the critical aspect ratio and aspect ratio of CNFs, respectively. The critical aspect ratio is related to the ratio of modulus/strength of filler to matrix and the composite dimensions as shown in Eq. (2), which obtained from the study of Vlasveld and coworkers [42].

$$\alpha_c = L_c/D = [(1 + \nu_m)\ln(2R/D)]^{1/2}(Y_f/Y_m)^{1/2} = K(Y_f/Y_m)^{1/2} \quad (2)$$

where ν_m is the poisson's ratio, R is the thickness of composite, D is the filler diameter/thickness, and K is a constant with value between 2 and 3 [43].

It was presumed that the aspect ratio, which could be calculated by length over diameter, would be the only difference for three types of CNFs. The following values were used for calculation: elastic modulus of CNFs (E_f) = 600 GPa, tensile strength of CNFs (F_f) = 8.7 GPa; elastic modulus of epoxy (E_m) = 16.4 GPa, tensile strength of epoxy (F_m) = 44.4 MPa. As shown in Fig. 9, the elastic modulus obtained by using the modified rule of mixture and the experimental data were in close agreement; furthermore, the tensile strength acquired from the modified rule of mixture was consistent with the experimental data for the nano-epoxy resins with 0.1% ECNFs-HDA, VGCNFs-HDA, and GCNFs-HDA. With increasing the mass fraction of three types of CNFs to 0.5%, the experimental results deviated from the theoretical values due to the non-uniformity in length of CNFs, non-uniform dispersion of CNFs, weak interfacial bonding strength between the filler and matrix, and filler agglomeration [44]. Additionally, the aspect ratio appeared to have significant effect on tensile strength when the mass fraction of filler was 0.5%; and the higher aspect ratio of CNFs was, the higher tensile strength would be. However, the aspect ratio did not show appreciable effect on elastic modulus.

3.3.2. Hybrid multi-scale CFRP composites made from the prepared nano-epoxy resins

The shear stress is typically transferred from layer to layer through resin matrix region during the inter-laminar shear failure and three-point flexural failure of the laminated composites. Hence, the main failure mechanism is related to the interfacial bonding strength; while the deformation/fracture of resin matrix may also contribute to the failure [45]. For impact properties, the impact absorption energy results in deformation of resin matrix, delamination of CFRP composites, and breakage and/or pull-out of fibers, which are also related to the interphase between fibers and resins. Therefore, to improve the mechanical properties of CFRP laminated composites, the interfacial bonding strength between matrix and filler and the properties of matrix have to be increased. In this study, the surfaces of three types of CNFs were functionalized by the linker molecule of HDA; this could also lead to the formation of chemical bonds between CNFs and epoxy resin. Therefore, the incorporation of HDA surface-functionalized CNFs into the epoxy resin could improve the property of composite resin matrix. In addition, the interfacial bonding strength would be enhanced due to the utilization of nano-epoxy resins. This is because the diameters of CNFs are 1–2 orders of magnitude smaller (*i.e.*, the specific surface areas of CNFs are 1–2 orders of magnitude larger) than those of conventional carbon fibers.

To further understand the reinforcement mechanism of HDA surface-functionalized CNFs (including ECNFs, VGCNFs, and GCNFs) in hybrid multi-scale CFRP composites, the fracture surfaces of three-point bending specimens were examined by SEM. The representative fracture surfaces of CFRP composites with 0.3% ECNFs-HDA, VGCNFs-HDA, and GCNFs-HDA, as well as the control sample, are shown in Fig. 10. The images on the left (A1, B1, C1, and D1) show the regions along the fiber direction, while the images on the right (A2, B2, C2, and D2) show the regions along the cross-sectional direction of fibers. For the control sample, the matrix detached from the surface of CFs due to weak interfacial bonding strength, and the failure surfaces of carbon fibers were relatively smooth without remnants of resin (Fig. 10A1 and A2). In comparison, the specimens with ECNFs-HDA, VGCNFs-HDA, and GCNFs-HDA could be distinguished from significantly different interfacial microstructures and the deformations of the resin matrices, as shown in Fig. 10B–D. These SEM micrographs showed that the CFs were surrounded by and/or adhered to the resin, indicating that the interfacial bonding strength between the CFs and the epoxy matrix was improved by the nano-epoxy resins containing ECNFs-HDA, VGCNFs-HDA, and GCNFs-HDA. Additionally, Fig. 10B1, C1, and D1 exhibited the dimpled/scalloped fracture feature. This could explain the formation of tougher interface between the epoxy matrix and CFs; and Fig. 10B2, C2, and D2 further confirmed that the interfacial bonding strength between the epoxy resin and CFs was improved due to the presence of closely arranged broken CFs. These results suggested that CNFs in the nano-epoxy

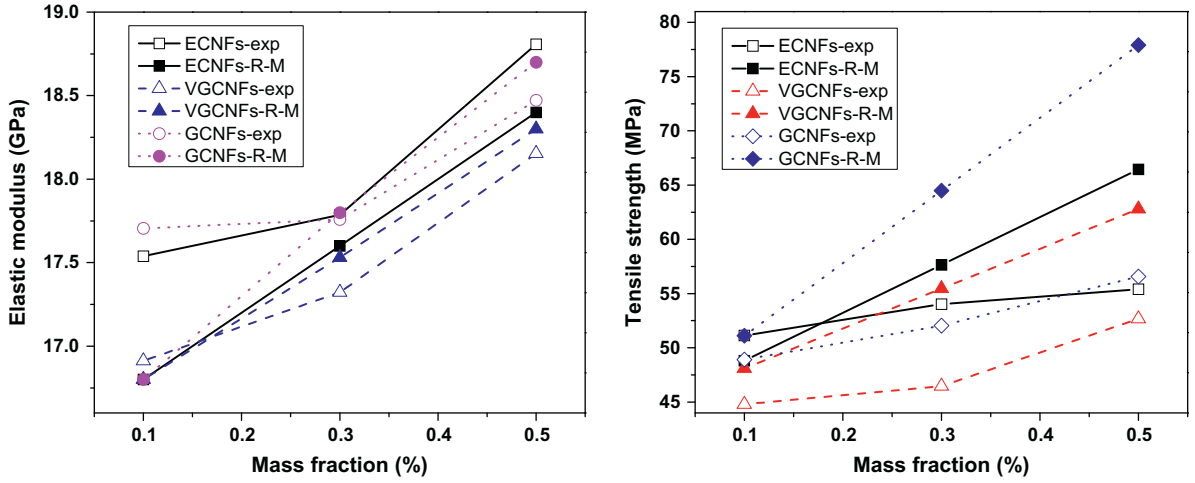

Fig. 9. Elastic modulus and tensile strength of nano-epoxy resins containing varied mass fractions of ECNFs-HDA, VGCNFs-HDA, or GCNFs-HDA. The mass fractions obtained from experiment (exp) were compared to those obtained from the modified rule of mixture equation (R–M).

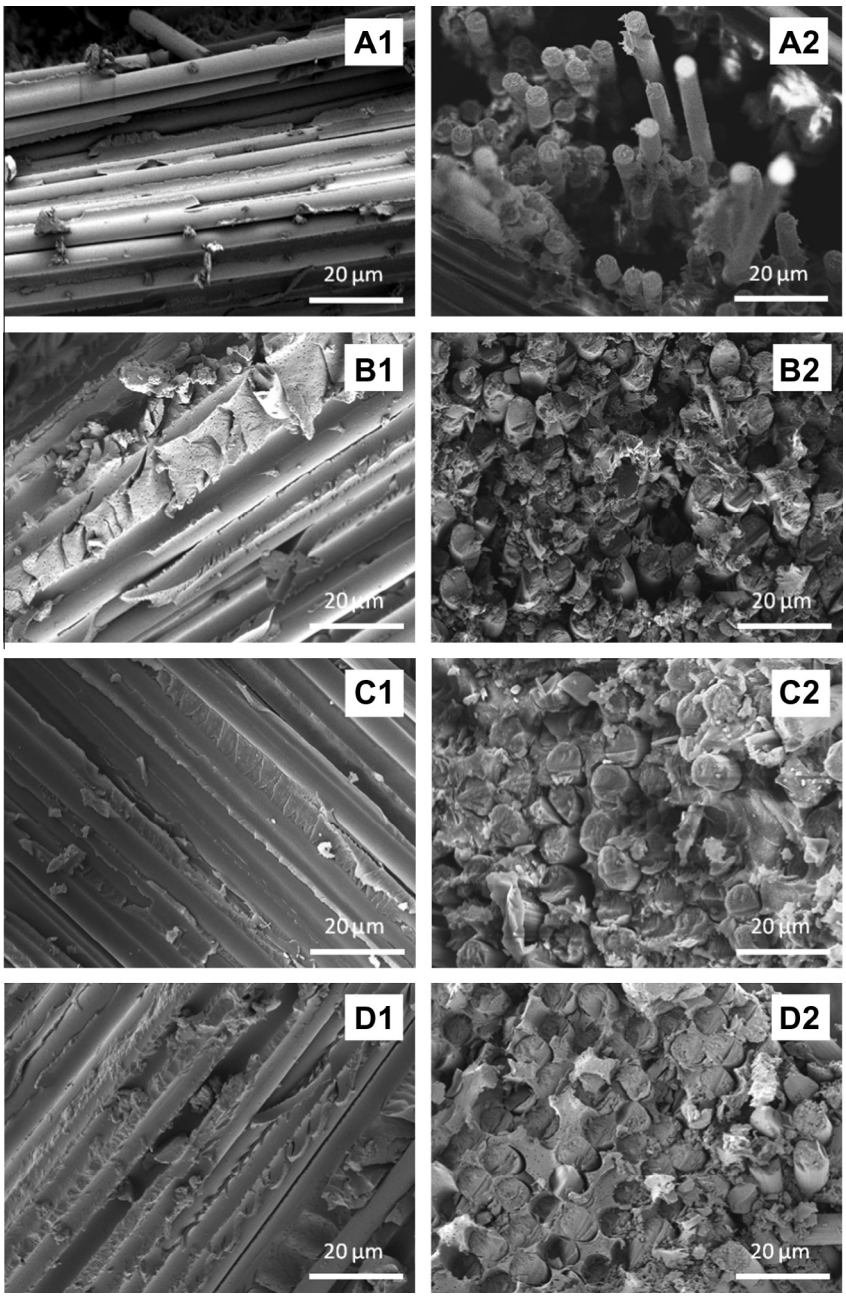

Fig. 10. SEM images showing the typical fracture surfaces acquired from three-point bending specimens: the control sample of CFRP composite without CNFs (A), and hybrid multi-scale CFRP composites containing 0.3% ECNFs-HDA (B), VGCNFs-HDA (C), and GCNFs-HDA (D). The images on the left (A1–D1) were taken along the fiber direction, while the images on the right (A2–D2) were taken along the direction perpendicular to the fibers.

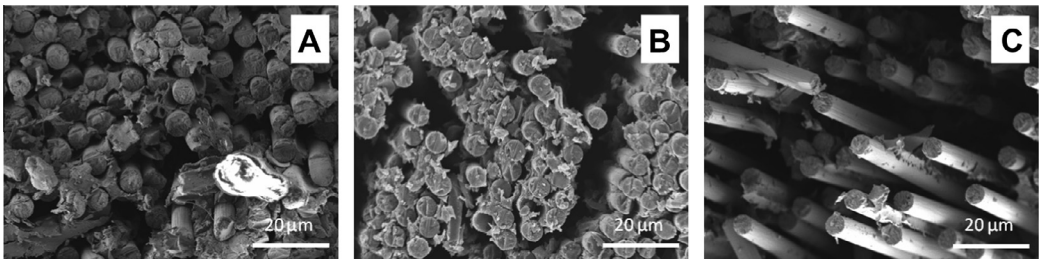

Fig. 11. SEM images showing the typical fracture surfaces acquired from three-point bending specimens of hybrid multi-scale CFRP composites containing 0.5% ECNFs-HDA (A), VGCNFs-HDA (B), and GCNFs-HDA (C).

resins could deflect micro-cracks, and thus the resistance to crack growth was increased, making the delamination more difficult to occur. Meanwhile, CNFs could also break and/or detach from the epoxy resin when the load was applied; this would increase the matrix deformation and dissipate the strain energy, further preventing the failure of composites and leading to the higher value of mechanical properties. Nonetheless, as shown in Fig. 11A–C, the CFs arranged less closely than those in Fig. 10B1, C1 and D1, while the CNFs appeared to form agglomerates during the VARTM process, indicating the incorporation of 0.5% ECNFs-HDA, VGCNFs-HDA, or GCNFs-HDA into epoxy resin could decrease the interfacial bonding strength between the epoxy resin and CFs. This was probably the reason that such composites had lower mechanical properties. For the nano-epoxy resins containing the same mass fraction of CNFs, they exhibited similar values of mechanical properties; however, the mechanical properties of GCNFs/CFRP composites were lower than those of ECNFs/CFRP and VGCNFs/CFRP composites. This was also due to the formation of GCNFs agglomerates, resulting in that the nano-epoxy resin could not be efficiently infused during the VARTM process to fabricate the composites, which would have the detrimental effect on the mechanical properties of composites consequently.

4. Concluding remarks

In this study, hybrid multi-scale composites were developed from woven fabrics of CFs and nano-epoxy resins containing short ECNFs (with diameters and lengths being ~200 nm and ~15 μm, respectively); for comparison, VGCNFs and GCNFs were also studied for the preparations of nano-epoxy resins and the corresponding hybrid multi-scale composites. It is noteworthy that, unlike VGCNFs and GCNFs that are prepared by bottom-up methods, ECNFs are produced through a top-down approach; hence, ECNFs are much more cost-effective than VGCNFs and GCNFs. The following remarks were concluded from experimental results:

(1) The nano-epoxy resins with ECNFs-HDA were prepared and evaluated for the first time. The incorporation of ECNFs-HDA into epoxy resin resulted in improvements on impact absorption energy, tensile strength, and flexural properties (strength, modulus, and work of fracture) simultaneously. Compared to the neat epoxy resin, the incorporation of 0.5% ECNFs-HDA resulted in the improvements of impact absorption energy by 17.3%, tensile strength by 22.5%, flexural strength by 10.0%, elastic modulus by 14.6%, and WOF by 43.7%, respectively.

(2) The aspect ratio of nanofibers had significant effect on strength but not on modulus of the resulting (cured) nano-epoxy resins. Regarding the improvements of impact, tensile, and flexural properties for the nano-epoxy resins, ECNFs outperformed VGCNFs and GCNFs.

(3) The prepared nano-epoxy resins were further studied to fabricate hybrid multi-scale CFRP composites *via* the VARTM technique. The study revealed that the nano-epoxy resins containing ECNFs-HDA, VGCNFs-HDA, or GCNFs-HDA led to improvements on impact absorption energy, inter-laminar shear strength, and flexural strength for the resulting hybrid multi-scale CFRP composites. This was due to the enhancement of interfacial bonding strength between composite resin matrix and CF filler as well as the improvement on mechanical properties of composite resin matrix.

(4) The three types of CNFs exhibited similar effects on the improvement of mechanical properties of the resulting hybrid multi-scale composites, whereas ECNFs and VGCNFs outperformed GCNFs slightly; this was because some agglomerates of GCNFs formed during the treatment process were too large to be infused during the fabrication of hybrid multi-scale composites, leading to lower mechanical properties.

(5) The optimal mass fraction of ECNFs-HDA, VGCNFs-HDA, and GCNFs-HDA in their nano-epoxy resins was identified to be 0.3%. The nano-epoxy resin with 0.3% ECNFs-HDA resulted in the improvements of impact absorption energy by 79.1%, inter-laminar shear strength by 42.2%, and flexural strength by 13.6%, respectively. When the mass fraction of ECNFs-HDA, VGCNFs-HDA, and GCNFs-HDA was higher (*e.g.*, 0.5%), the agglomerates of nanofibers would be formed or the nanofibers would be filtered out by CF fabrics; these would result in the decrease of mechanical properties.

(6) This study suggested that ECNFs had the potential to be utilized as innovative reinforcement agent for the development of nano-epoxy resins, which could be further utilized for the fabrication of high-performance laminated composites.

Acknowledgments

This research was supported by the National Aeronautics and Space Administration (NASA) of the U.S. under the Grant Number of NNX07AT52A, the U.S. Air Force Research Laboratory (AFRL) under the Cooperative Agreement Number of FA9453-06-C-0366, and the National Natural Science Foundation of China (NSFC) under the Grant Number of 51273010.

References

[1] Luo JJ, Daniel IM. Characterization and modeling of mechanical behavior of polymer/clay nanocomposites. Compos Sci Technol 2003;63(11):1607–16.
[2] Li J, Vergne MJ, Mowles ED, Zhong WH, Hercules DM, Lukehart CM. Surface functionalization and characterization of graphitic carbon nanofibers (GCNFs). Carbon 2005;43:2883–93.
[3] Hammel E, Tang X, Trampert M, Schmitt T, Mauthner K, Eder A, et al. Carbon nanofibers for composite applications. Carbon 2004;42:1153–8.
[4] Tibbetts GG, Lake ML, Strong KL, Rice BP. A review of the fabrication and properties of vapor-grown carbon nanofibers/polymer composites. Compos Sci Technol 2007;67:1709–18.
[5] Kim JA, Seong DG, Kang TJ, Youn JR. Effects of surface modification on rheological and mechanical properties of CNT/epoxy composites. Carbon 2006;44:1898–906.
[6] Zhu J, Wei S, Ryu J, Budhathoki M, Liang G, Guo Z. In situ stabilized carbon nanofiber (CNF) reinforced epoxy nanocomposites. J Mater Chem 2010;20:4937–48.
[7] Gojny FH, Nastalczyk J, Roslaniec Z, Schulte K. Surface modified multi-walled carbon nanotubes in CNT/epoxy composites. Chem Phys Lett 2003;370:820–4.
[8] Yang Z, McElrath K, Bahr J, D'Souza NA. Effect of matrix glass transition on reinforcement efficiency of epoxy-matrix composites with single walled carbon nanotubes, multi-walled carbon nanotubes, carbon nanofibers and graphite. Composites Part B 2012;43:2079–86.
[9] Karsli NG, Aytac A. Tensile and thermomechanical properties of short carbon fiber reinforced polyamide 6 composites. Composites Part B 2013;51:270–5.
[10] Gacia EJ, Wardle BL, Hart AJ. Joining prepreg composite interfaces with aligned carbon nanotubes. Composites Part A 2008;39:1065–70.
[11] Lu M, He B, Wang L, Ge W, Lu Q, Liu Y, et al. Preparation of polystyrene–polyisoprene core–shell nanoparticles for reinforcement of elastomers. Composites Part B 2012;43:50–6.
[12] Gojny FH, Wichmann MHG, Fiedler B. Influence of nano-modification on the mechanical and electrical properties of conventional fiber-reinforced composites. Composites Part A 2005;36:1525–35.
[13] Wichmann MHG, Sumfleth J, Gojny FH. Glass fiber-reinforced composites with enhanced mechanical and electrical properties-benefits and limitations of a nanoparticles modified matrix. Eng Fract Mech 2006;73:2346–59.
[14] Thostenson ET, Li WZ, Wang DZ, Ren ZF, Chou TW. Carbon nanotubes/carbon fiber hybrid multiscale composites. J Appl Phys 2002;91:6034–7.
[15] Tsai JL, Wu MD. Organoclay effect on mechanical response of glass/epoxy nanocomposites. J Compos Mater 2008;42(6):553–68.
[16] Moradpour R, Taheri-Nassaj E, Parhizkar T, Ghodsian M. The effects of nanoscale expansive agents on the mechanical properties of non-shrink cement-based composites: The influence of nano-MgO addition. Composites Part B 2013;55:193–202.

[17] Davis DC, Whelan BD. An experimental study of interlaminar shear fracture toughness of a nanotube reinforced composite. Composites Part B 2011;42:105–16.
[18] Park JK, Do IH, Askeland P. Electrodeposition of exfoliated graphite nanoparticles onto carbon fibers and properties of their epoxy composites. Compos Sci Technol 2008;68:1734–41.
[19] Allaoui A, Bai S, Cheng HM. Mechanical and electrical properties of a MWNT/epoxy composites. Compos Sci Technol 2002;62:1993–8.
[20] Kinloch AJ, Masania K, Taylor AC. The fracture of glass-fiber-reinforced epoxy composites using nanoparticle-modified matrices. J Mater Sci 2008;43:1151–4.
[21] Zhou Y, Pervin F, Rangari V, Jeelani S. Fabrication and evaluation of carbon nanofiber filled carbon/epoxy composite. Mater Sci Eng A 2006;426(1–2):221–8.
[22] Kim M, Park Y, Okoli O, Zhang C. Processing, characterization, and modeling of carbon nanotube-reinforced multiscale composites. Compos Sci Technol 2009;69(1–2):335–42.
[23] Zhou Y, Hosur M, Jeelani S, Mallick P. Fabrication and characterization of carbon fiber reinforced clay/epoxy composite. J Mater Sci 2012;47:5002–12.
[24] Qiu J, Zhang C, Wang B, Liang R. Carbon nanotube integrated multifunctional multiscale composites. Nanotechnology 2007;18(27):1–11.
[25] Chen Q, Zhang LF, Zhao Y, Wu XF, Fong H. Hybrid multi-scale composites developed from glass microfiber fabrics and nano-epoxy resins containing electrospun glass nanofibers. Composites Part B 2012;43:309–16.
[26] Huang ZM, Zhang YZ, Kotaki M, Ramakrishna S. A review on polymer nanofibers by electrospinning and their applications in nanocomposites. Compos Sci Technol 2003;63:2223–53.
[27] Chen Q, Zhang LF, Yoon MK, Wu XF, Arefin RH, Fong H. Preparation and evaluation of nano-epoxy composite resins containing electrospun glass nanofibers. J Appl Polym Sci 2012;124:444–51.
[28] Fong H. Electrospun nylon 6 nanofiber reinforced Bis-GMA/TEGDMA dental restorative composite resins. Polymer 2004;45:2427–32.
[29] Dzenis Y. Spinning continuous fibers for nanotechnology. Science 2004;304:1917–9.
[30] Chen Q, Zhang LF, Rahman A, Zhou ZP, Wu XF, Fong H. Hybrid multi-scale epoxy composite made of conventional carbon fiber fabrics with interlaminar regions containing electrospun carbon nanofiber mats. Composites Part A 2011;42:2036–42.
[31] Chen Q, Zhao Y, Zhou ZP, Rahman A, Wu XF, Wu WD, et al. Fabrication and mechanical properties of hybrid multi-scale epoxy composites reinforced with conventional carbon fiber fabrics surface-attached with electrospun carbon nanofibers mats. Composites Part B 2013;44:1–7.
[32] Lourie O, Cox DE, Wagner HD. Buckling and collapse of embedded carbon nanotubes. Phys Rev Lett 1998;81:1638–41.
[33] Thess A, Lee R, Nikolaev P, Dai H, Petit P, Robert J. Crystalline ropes of metallic carbon nanotubes. Science 1996;273:483–7.
[34] Eineli Y, Koch VR. Chemical oxidation: a route to enhanced capacity in Li-ion graphite anodes. J Electrochem Soc 1997;144:2968–73.
[35] Hamon MA, Chen J, Hu H, Chen YS, Itkis ME, Rao AM. Dissolution of single-walled carbon nanotubes. Adv Mater 1999;11:834–40.
[36] Inam F, Wong D, Kuwata M, Peijs T. Multiscale hybrid micro-nanocomposites based on carbon nanotubes and carbon fibers. J Nanomater 2010:12. Article ID 453420.
[37] Calvert P. Nanotube composites – a recipe for strength. Nature 1999;399:210–1.
[38] Piggott MR. Why interface testing by single-fiber methods can be misleading. Compos Sci Technol 1997;57:965–74.
[39] Kalantar J, Drzal LT. The bonding mechanism of aramid fibers to epoxy matrices. J Mater Sci 1990;25:4186–93.
[40] Xu RL, Bhamidipati V, Zhong WH, Li J, Lukehart CM. Mechanical property characterization of a polymeric nanocomposite reinforced by graphitic nanofibers with reactive linkers. J Compos Mater 2004;38:1563–82.
[41] Shi DL, Feng XQ, Huang YY, Hwang KC. The effect of nanotubes waviness and agglomeration on the elastic property on carbon nanotubes-reinforced composites. J Eng Mater Technol 2004;126:250–7.
[42] Longun J, Iroh JO. Nano-graphene/polyimide composites with extremely high rubbery plateau modulus. Carbon 2012;50:1823–32.
[43] Vlasvelda DPN, Parlevliet PP, Bersee HEN, Picken SJ. Fiber-matrix adhesion in glass-fiber reinforced polyamide-6 silicate nanocomposites. Composites Part A 2005;36:1–11.
[44] Fornes TD, Paul DR. Modeling properties of nylon 6/clay nanocomposites using composite theories. Polymer 2003;44:4993–5013.
[45] Zhu J, Imam A, Crane R. Processing a glass fiber reinforced vinyl ester composite with nanotubes enhancement of interlaminar shear strength. Compos Sci Technol 2007;67:1509–17.